

MEASUREMENTS OF T_0 TEMPERATURES OF SUPERSATURATED Si-As ALLOYS

Kwang-Ryeol Lee*, Jeffrey A. West*, Patrick M. Smith*, M. J. Aziz* and J. A. Knapp**

* Harvard University, Division of Applied Sciences, Cambridge, MA 02138.

** Sandia National Laboratories, Albuquerque, NM 87158.

ABSTRACT

The congruent melting point, or T_0 curve, of crystalline Si-As alloys has been measured in the range of 1.6 to 18.1 at. % arsenic by line source electron beam annealing. Alloys were created by ion implantation of As into 0.1mm Si-on-sapphire and crystallized by pulsed laser melting. T_0 temperatures decrease from $1673 \pm 10\text{K}$ at 2.0 at.% As to $1516 \pm 30\text{K}$ at 18.1 at.% As. The results of these measurements are significantly higher than the previous results of studies using pulsed laser melting techniques. Advantages of the e-beam technique over previous techniques are discussed. Chemical free energy functions of the solid and liquid phases were calculated from existing thermodynamic data. The calculated T_0 curve agrees with the measured values only in low concentration region (less than 8 at.%).

INTRODUCTION

A quantitative experimental test of theories for nonequilibrium interface kinetics during alloy solidification [1] requires, as input, reliable thermodynamic functions for the liquid and solid phases. The Si-As system is a promising one for such a test because of the ease with which the solidification velocity and the nonequilibrium partition coefficient can be measured in Si alloys, and because of the high solubility of As in Si [2] and the large supersaturations that can be obtained in this system by rapid solidification [3]. Although As is one of the important dopants of Si, however, thermodynamic data in this system are insufficient and often inconsistent [4-9]. One example is the T_0 curve, the temperature at which solid and liquid phases of equal composition have equal Gibbs free energies. Recently, pulsed laser melting experiments have been used to determine the T_0 temperatures of supersaturated Si-As alloys [8,9]. The T_0 temperatures reported in these experiments differ from each other by more than 200 degrees. Solid solubility data also contradict each other [4].

In order to obtain a useful thermodynamic constraint on the free energy functions, we re-measured the T_0 temperatures. Supersaturated Si-As alloy films on sapphire substrates were prepared by rapid melting and solidification with a pulsed excimer laser. Line source e-beam annealing (LEBA) was used for melting the alloy films [10-12]. The heating rate by e-beam irradiation is fast enough to suppress melting when partitioning is required, such as the solidus temperature is surpassed. Rather, melting initiates when the T_0 temperature is reached and partitionless melting becomes possible. The LEBA experiment has several advantages over pulsed laser experiments. First, electrons are not reflected from the specimen surface, so accurate data on the reflectivity and on the reflectivity change upon melting are not required for a reliable calculation of the energy deposition. Second, the time scale of the e-beam heating experiment is on the order of 100 μs . The deposited energy can spread to greater depths in this amount of time. Therefore, the absorption depth is not important. Furthermore, the alloy films used in this work are thin enough (100nm) that their effect on the e-beam energy deposition and thermal diffusion is negligible. For example, heat flow calculations indicate that the temperature difference across the alloy layer is less than 1 degree. Hence the temperature of the Si-As film can safely be assumed to equal that of sapphire substrate at the boundary. Consequently, the temperature history can be calculated by using only the physical data of sapphire, which are well known [10,11], and the e-beam parameters. These advantages make it possible to obtain more reliable T_0 temperatures than in laser melting experiments [8,9].

EXPERIMENTAL RESULTS

Silicon films of 100 nm thickness on sapphire substrates were implanted with 60keV $^{75}\text{As}^+$ ions at various doses from 1×10^{16} to $8 \times 10^{16}/\text{cm}^2$. Samples were covered by a mask during the

implantation to make alternating stripes of Si-As alloy and pure Si, as shown in Fig.1. This sample geometry embedded a standard (pure Si) into each sample for e-beam power calibration. The implanted regions in these samples were all amorphous and had non-uniform As depth profiles. XeCl excimer laser pulses (40ns pulse duration, 308nm wavelength) were used to homogenize and crystallize the samples. The samples were melted from 5 to 15 times depending on the implant dose. The energy density of the laser pulse was selected to melt barely to the back of the film in order to avoid possible damage due to liquid overheating or long melt duration. Transient conductance and reflectance measurements were performed to record the melt history on a companion set of TCM-patterned, otherwise-identical samples. After pulsed laser melting, the As concentration profiles were measured by Rutherford Backscattering Spectrometry (RBS) in grazing-exit geometry. The microstructure of one laser melted sample was observed in cross-sectional TEM to confirm that the resulting material is crystalline single phase, and to examine the density of crystal defects.

Low dose samples (1×10^{16} and $2 \times 10^{16}/\text{cm}^2$) were crystallized and homogenized by melting and regrowth during the laser irradiation. It was observed that after the laser irradiation, the electric conductance increases and the color of the sample surface changes due to crystallization. However, high dose samples ($7 \times 10^{16}/\text{cm}^2$ and $8 \times 10^{16}/\text{cm}^2$) regrew as amorphous after full melting. These samples were homogenized by a number of melting and regrowth cycles, and then explosively crystallized at low energy densities. Cross-sectional TEM of one explosively crystallized sample (dose: $6 \times 10^{16}/\text{cm}^2$) revealed single phase material with fine grains of about 50nm diameter, as seen in previous studies on explosive crystallization in pure Si [13]. Samples with the intermediate dose of $4 \times 10^{16}/\text{cm}^2$ seemed to solidify partly crystalline and partly amorphous as judged by optical inspection. We subsequently used the same explosive crystallization technique as in high dose samples to fully crystallize these samples. The compositions of As in the homogenized samples are shown in Table 1. The final composition-depth profiles never displayed nonuniformities greater than ± 2 at. %.

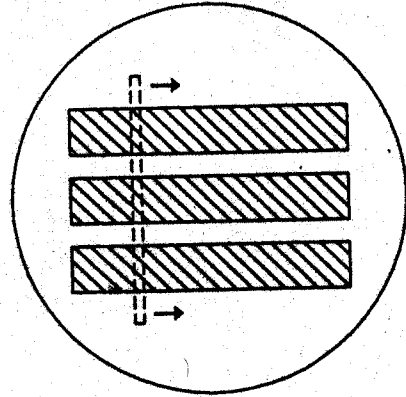


Figure.1. Schematic plan view of the sample. Alternating stripes of implanted region (hatched area) and pure Si were made using a mask during implantation. E-beam (broken rectangle) swept the sample in direction of arrow.

Dose ($\times 10^{16}/\text{cm}^2$)	Conc.(at.%)	T_m (K)
1	2.0 ± 0.5	1673 ± 10
2	4.0 ± 0.5	1660 ± 10
4	8.1 ± 0.6	1593 ± 30
7	14.5 ± 2.0	1545 ± 30
8	18.1 ± 1.0	1516 ± 30

Table 1. Specimen compositions and measured T_o temperatures.

A line source e-beam (20mm long x 1mm wide) was used to heat these samples rapidly to a known peak temperature. The e-beam source and annealing system are described in detail elsewhere [10-12]. Since the thermal properties of sapphire and the e-beam parameters are accurately known or measured, the temperature profile along the e-beam sweep could be calculated to within 10 degrees. The e-beam was swept along the implantation stripe as shown in Fig. 1. Hence, the e-beam could sweep Si-As alloy stripes and pure Si stripes simultaneously. The microstructure of the e-beam melted region is distinctly different from that of the unmelted regions. The e-beam power used in the temperature profile calculation was calibrated using the melt width in the pure Si stripes. The T_0 temperature was then determined by comparing the melt width of the alloy stripe with the calculated temperature profile.

Measured T_0 temperatures of supersaturated Si-As alloys are shown in column 3 of Table 1. Low dose samples (1×10^{16} and $2 \times 10^{16}/\text{cm}^2$) were crystallized directly by regrowth from the melt. These samples are thus expected to have large grains even though they contain some defects. The measured T_0 values are thus highly reliable in the low As concentration region. However, since the high dose samples ($\geq 4 \times 10^{16}/\text{cm}^2$) were crystallized by explosive crystallization resulting in a fine polycrystalline microstructure, the T_0 values from these samples remain preliminary until the effect of the microstructure on the T_0 value is investigated. We have found that, depending on laser conditions, the $2 \times 10^{16}/\text{cm}^2$ samples can be either solidified in the crystalline state or solidified in the amorphous state and subsequently explosively crystallized. The T_0 temperatures of these alloys will be compared to each other in order to determine whether there is any effect on the apparent T_0 values due to the fine-grained microstructure that results from explosive crystallization.

DISCUSSION

The T_0 temperatures measured in this work are summarized in Fig. 2 as a function of As concentration. Results from the pulsed laser melting experiments are also shown in Fig. 2. Baeri *et al.* [8] found much lower T_0 temperatures than this work. They measured the threshold energy densities for melting by a pulsed ruby laser and then calculated the specimen surface temperature. This calculation required optical and thermal parameters such as reflectivity, absorption coefficient, heat capacity, and thermal diffusivity. For laser melting in the nanosecond time regime, the details of laser energy deposition and temperature gradients in the surface alloy layer are very important for calculations of the temperature profile. However, in the absence of thermophysical data, assumptions had to be made about the dependencies of these parameters on temperature and solute concentration. In the other pulsed laser experiment, Peercy *et al.* estimated the T_0 temperature from the retardation of solidification near the As peak in As-implanted Si on sapphire samples [9]; they also found T_0 temperatures lower than, but much closer to, ours. Although the laser energy deposition did not affect their results, assumptions had to be made about the composition dependence of thermal properties of the alloy in their calculation. The uncertainties in the thermal and optical properties of Si-As alloys should be considered the main reason for the inaccurate estimation of T_0 values in both previous studies.

This measurement of the T_0 curve can be used as a constraint on thermodynamic modeling of the solid and liquid phases in these alloys. We derived the free energy functions of each phase from existing thermodynamic data. The validity of the thermodynamic model will be tested by comparing calculated T_0 curves with the measured values. We assumed a quasi-regular solution model (the interaction parameter was allowed to depend linearly on temperature but not on composition) for both the solid and liquid phases. With the diamond cubic phases of pure Si and pure As chosen as the reference states, the molar Gibbs free energy for each phase can then be written

$$G_m^s = RT [(1-x_s) \ln (1-x_s) + x_s \ln (x_s)] + x_s (1-x_s) \Omega_s \quad (1)$$

$$G_m^l = (1-x_l) \Delta G^{\circ}_{Si(d \rightarrow l)} + x_l \Delta G^{\circ}_{As(d \rightarrow l)} \\ + RT [(1-x_l) \ln (1-x_l) + x_l \ln (x_l)] + x_l (1-x_l) \Omega_l \quad (2)$$

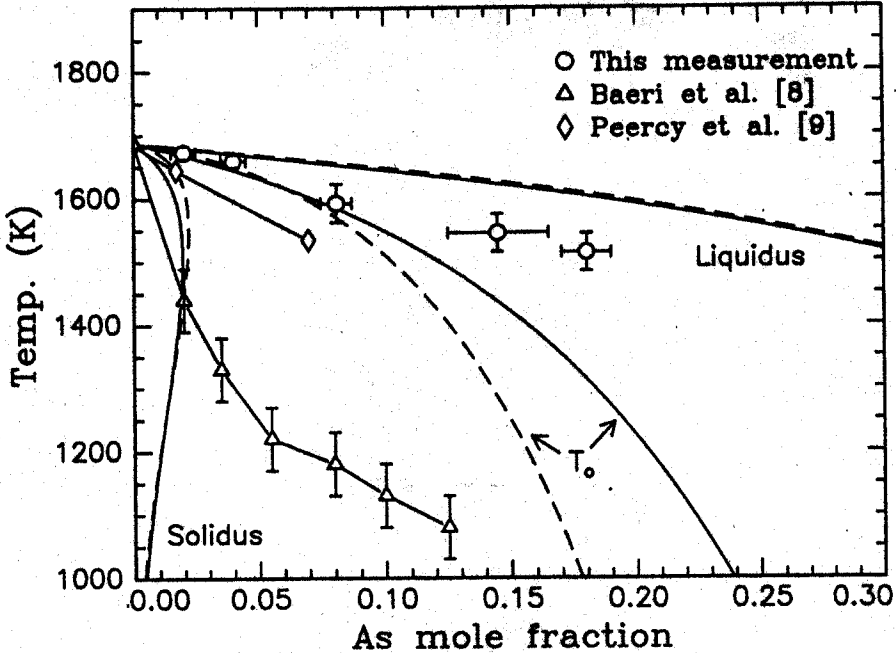


Figure 2. Measured T_0 temperatures and calculated phase boundaries and T_0 curve in Si-As alloys. Solid curves are calculated phase boundaries and T_0 curve when $T_{m(As,d)}=0K$, and broken curves are those when $T_{m(As,d)}=-5000K$.

Here, x_i is the mole fraction of As in phase i , R the gas constant, and T the temperature in K. The "lattice stability" of pure Si, $\Delta G^\circ_{Si(d \rightarrow l)}$, is known [14]. The unknown "lattice stability" of pure diamond cubic As, $\Delta G^\circ_{As(d \rightarrow l)}$, was estimated by assuming that the melting temperature of pure diamond cubic As would be in the range from 0K to -5000K, and that the entropy of fusion is the same as for pure Si. The thermodynamic calculations reported here were done using both 0K and -5000K for the melting temperature of diamond cubic As to provide reasonable estimates of upper and lower limits on the calculated T_0 values. The interaction parameters of each phase, Ω_s and Ω_l , were obtained by fitting to the activity coefficients of As in Si-As solid solutions [15,16] and to the experimental liquidus data [4,17], respectively. The thermodynamic parameters obtained as linear functions of temperature are listed in Table 2.

The solid and broken lines in Fig.2 are the calculated phase boundaries and T_0 curves when 0K and -5000K, respectively, are used as the melting temperature of diamond cubic As. The calculated phase boundaries and T_0 curve in the low concentration region are not sensitive to the uncertainty in the As lattice stability. However, the T_0 curves become more sensitive to such uncertainty at higher As concentrations. The calculated T_0 curve agrees with our measurements for As concentrations less than 8 at.%. Beyond this composition, the calculated T_0 temperature decreases faster than the measured T_0 temperatures. Although the measured values in the high concentration region are preliminary, it is anticipated that any "microstructure correction" would only raise these data points to higher values, so it is unlikely that agreement with the model will result. One possible reason for the deviation in the high As concentration region is that the available thermodynamic data are insufficient. For example, the activity coefficient of As in Si-As solid solutions was measured only at low concentrations (maximum 3 at. % As) [15,16].

	$T_{m(As,d)} = 0K$	$T_{m(As,d)} = -5000K$
$\Delta G^\circ_{Si(d \rightarrow l)}$	50626 - 30T	50626 - 30T
$\Delta G^\circ_{As(d \rightarrow l)}$	-30T	-149257 - 30T
Ω_2	34572 - 34T	-98116 - 50T
Ω_1	124793 - 100T	124793 - 100T

Table 2. Calculated thermodynamic parameters of Si-As alloy in J/mole.
(T is the temperature in K)

Extrapolation of this data into the high concentration range may cause large errors. Another possible reason is that the thermodynamic model used in this work is too simple to consider the thermodynamic behavior in the high concentration regime. However, a model with more free parameters also requires more thermodynamic data to determine them.

CONCLUSIONS

The combination of rapid quenching by pulsed laser melting and sufficiently rapid heating by electron-beam irradiation provide a useful technique to measure the T_0 temperature of supersaturated alloys. The use of the e-beam melting technique with thin alloy film samples has the important advantage that the thermophysical properties of the alloy layer and the e-beam parameters are not important for the temperature calculation. We observe higher T_0 temperatures for the Si-As system than do previous experiments [8,9].

The T_0 curve was calculated using available thermodynamic data for dilute alloys. This calculation agrees with the measured data in the low As concentration region. However, the calculations predict lower T_0 temperatures than are measured for high As concentrations. Further studies are in progress to obtain a thermodynamic model valid over the entire composition range.

ACKNOWLEDGEMENT

The authors are grateful to M. O. Thompson for the phase diagram calculation program. One of the authors (K.-R. Lee) received financial support from the Korea Science and Engineering Foundation during his study at Harvard University. Work at Harvard was supported by NSF-PYIA Program (B.A. MacDonald). Work performed at Sandia was supported by the US Department of Energy, contract number DE-AC04-76DP00789.

REFERENCES

1. M.J. Aziz and T. Kaplan, *Acta Metall.* **36**, 2335 (1988).
2. F.A. Trumbore, *Bell Sys. Tech. J.* **1960** (1), 205.
3. C.W. White, S.R. Wilson, B.R. Appleton and F.W. Young, Jr., *J. Appl. Phys.* **51**, 738 (1980).
4. R.W. Olesinski and G.J. Abbaschian, *Bull. Alloy Phase Diagrams* **8** (3), 254 (1985).
5. R.B. Fair and G.R. Weber, *J. Appl. Phys.* **44**, 273 (1973).
6. A. Lietoila, J.F. Gibbons, T.J. Magee, J. Peng and J. D. Hong, *Appl. Phys. Lett.* **35**, 532 (1979).

7. N. Miyamoto, E. Kuroda and S. Yoshida, *J. Jpn. Soc. Appl. Phys., Suppl.* **43**, 408 (1974).
8. P. Baeri, R. Reitano, A.M. Malvezzi and A. Borghesi, *J. Appl. Phys.* **67** (4), 1801 (1990).
9. P.S. Peercy, M.O. Thompson, and J.Y. Tsao, *Appl. Phys. Lett.* **47** (3), 244 (1985).
10. J.A. Knapp, *J. Appl. Phys.* **58** (7), 2584 (1985).
11. J.A. Knapp and D.M. Follstaedt, *Phys. Rev. Lett.* **58** (23), 2454 (1987).
12. D.M. Follstaedt and J.A. Knapp, *Mater. Res. Soc. Proc.* **100**, 597 (1988).
13. J. Narayan, C.W. White, M.J. Aziz, B. Stritzker and A. Walthuis, *J. Appl. Phys.* **57** (2), 564 (1985).
14. Thermodynamic Properties of Inorganic Substances, edited by I. Barin and O. Kancke (Springer-Verlag, New York, 1973) p. 674.
15. J.S. Sandhu and J.L. Reuter, *IBM J. Res. Develop.* **16** (11), 464 (1971).
16. V.I. Belousov, *Russian J. of Physical Chemistry*, **53** (9), 1266 (1979).
17. W. Klemm and P. Pirscher, *Z. Anorg. Chem.* **247**, 211 (1941)